JOURNAL OF RESEARCH of the National Bureau of Standards—Engineering and Instrumentation
Vol. 64C, No. 3, July–September 1960

Variation of Resolving Power and Type of Test Pattern

Francis E. Washer and William P. Tayman

(April 7, 1960)

The plane of best average definition is located for a number of lenses of a type used in airplane mapping cameras. Three different types of test pattern are used for each lens. These patterns are the long-line, short-line, and annulus. Results of measurement that show the variation of resolving power throughout the region of usable imagery are given for each type of test pattern with two types of photographic emulsion. It is found that the plane of best average definition can be located equally well with each type of pattern. There are, however, pronounced differences in the numerical magnitudes of the values of resolving power determined with the various types of test pattern. In general, the highest values are attained with the long-line patterns. Values of the various rating indices $\sqrt{R_\beta T_\beta}$, AWAR, and ADWAR are given together with a comparison of the different order of merit assigned by these indices.

1. Introduction

The quality of definition throughout the image plane of lenses used in airplane mapping cameras is of prime importance in ensuring satisfactory photography upon which to base the compilation of reliable maps. In forming an estimate of the probable quality of definition for a given lens, it is customary to use the measured values of resolving power for specified areas of the image plane as the principal criterion upon which to base the estimate.

The measured values of the resolving power have in general proved satisfactory for locating the plane of best average definition and for determining the suitability of a given lens for use in an aerial camera. Consequently, most specifications dealing with aerial cameras contain requirements prescribing the minimum acceptable values of the resolving power. Unfortunately, there is marked variance in the type of test chart used in various laboratories and in the conditions of use. This variance is a source of difficulty in any attempt to formulate an international specification dealing with the calibration of photogrammetric cameras as was done at the Washington meeting of the International Society of Photogrammetry in 1952 [1].[1] To obviate the difficulty, a specification was adopted for trial and discussion that permitted the use of several different types of resolving power target. It was noted that it was not possible at the time to standardize on a single type of resolving power target.

Three types of test chart were included in this tentative specification which were the three-line target used by the U.S. Air Force [2], the Cobb two-line chart used in Great Britain [3], and the annulus chart used in Canada [4]. All of these charts were of low contrast except the three-line chart of the Air Force which included both high- and low-contrast versions. The three-line chart used by the National Bureau of Standards was not included, as it had been in existence for only a few months prior to the conference, and its properties were not widely known.

Each of the charts covered by the specification included a series of patterns whose sizes were in a geometric progression with the $\sqrt[6]{2}$ preferred for the common ratio between adjacent pattern sizes. The NBS chart of 1952 not only differed from the others in length of line but also in the ratio between successive pattern sizes which is $\sqrt[4]{2}$.

In the seven years that have passed since the adoption of this specification, agreement on a single type of chart has not yet developed. A few publications have appeared [5, 6] that permit an estimate of the differences in resolving power likely to be found for line charts compared with annulus charts.

Because of some of the differences that exist between the procedures recommended for the calibration of photogrammetric cameras and those used at the National Bureau of Standards, it is worthwhile to describe the methods used at the Bureau and to compare the results derived therefrom with those that would be obtained by the methods approved in the international standard. In the present paper measured values of resolving power obtained with the NBS chart of 1952 [7] are compared with those obtained with the three-line chart used by the U.S. Air Force and with an annulus chart which differs from that prescribed in the international specification in that it is a high-contrast instead of a low-contrast target. In addition, the size ratio for successive patterns in each type of target is $\sqrt[4]{2}$ instead of $\sqrt[6]{2}$.

Results are presented for six lenses using two types of emulsion. Values of the several indices that might be used as rating factors such as $\sqrt{R_\beta T_\beta}$, AWAR, and ADWAR are compared. It is found that the plane of best average definition may be located equally well with any of the three types. Values of resolving power obtained with the NBS chart are usually higher than those obtained with the other charts.

[1] Figures in brackets indicate the literature references at the end of this paper.

2. Method of Measurement

2.1. Test Camera

The National Bureau of Standards precision lens testing camera [8] was used in making the negatives from which the values of resolving power are determined. This device is well adapted for use in locating the plane of best average definition of a lens. Its construction and mode of operation simplifies the process of evaluating the resolving power of a lens in a series of focal planes spaced at definite intervals along the optical axis. Moreover, by using one type of chart in the odd-numbered collimators and another type in the even-numbered collimators, it is possible to register the imagery in the same identical series of focal planes for each type of chart for the same series of angular separations β from the axis on the same plate.

2.2. Test Charts

Three distinct types of test charts are used in the present investigation. All three are high-contrast charts, i.e., the difference in optical density between line and background exceeds 2.0. Each chart consists of a suitable range of sizes of the test object with the size proceeding in a geometric progression with $\sqrt[4]{2}$ (or 1.1892) as the common ratio. The various types of test chart are described in the following sections.

a. NBS Resolution Test Chart of 1952

This chart was introduced in 1952 and is described in detail in NBS Circular 533. The test chart, shown in figure 1, is a composite chart prepared by superimposing one test chart upon a four-times enlargement of the same chart. In this chart, all patterns have the same line count, namely three to each group. Two series of test patterns are included

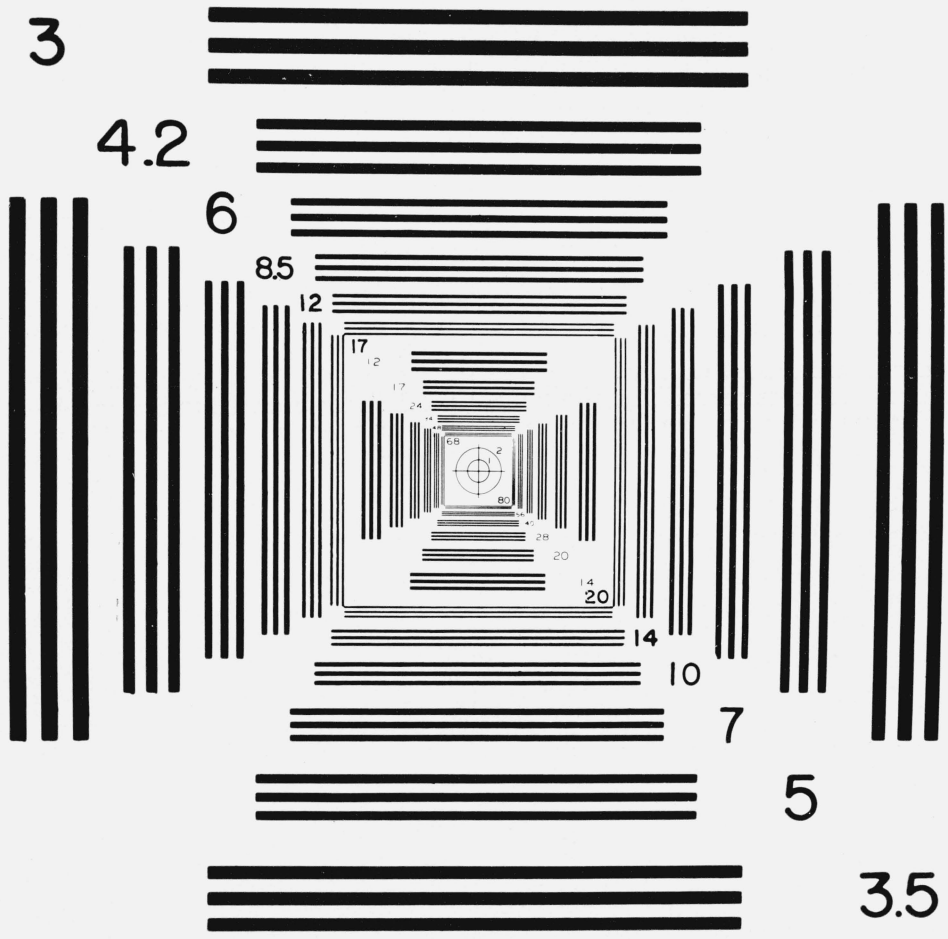

FIGURE 1. *NBS long-line resolution chart with extended range.*

This chart is a composite formed by superposing the NBS standard test chart upon a 4× enlarged copy of the master chart. The ratio of line spacings in adjacent groups of the master chart is equal to $\sqrt{2}$; however, the ratio of the line spacings of corresponding opposite patterns is $\sqrt[4]{2}$. Consequently, for this extended range chart, the values of resolving power that can be measured for a lens of 6-in. focal length range from 6.3 to 168 lines/mm. in a geometric series proceeding by $\sqrt[4]{2}$.

such that the spacings in the line pattern of a given group differ from those in the adjacent group in the ratio of $\sqrt[4]{2}$. However, the spacing in the initial pattern of one series differs from the initial pattern of the other series by $\sqrt[4]{2}$. Consequently, considered as a whole, the range of values provided by this chart proceeds by the $\sqrt[4]{2}$. The size of the chart used as a reticle in the collimators of the lens testing camera for this study was such that the range of values in the image plane of the lenses investigated extends from 6.3 to 168 lines/mm. The most striking feature of this chart is the relatively great length of the lines forming the patterns. The ratio of length to width of line is sufficiently great that the visual resolving power as read will not be subject to variations arising from end effects, and the images will continue to look like lines down to the limit of resolution. The ratio is also sufficiently great that the variation of resolving power with ratio of length to width of line can be neglected [5]. In addition, both the original test pattern and the images on a negative formed by a lens can be readily scanned with a recording microdensitometer. This property permits the user to make accurate measurements of the contrast between line and space for both object and image for studies involving degradation of contrast for a particular lens-emulsion combination.

The same size test chart is used in the various collimators so that it is necessary to apply the "cosine" and "cosine-squared" corrections to images formed off-axis.

b. Short Three-Line Charts

These charts, shown in figure 2, were adapted from that used in the camera calibrator [9]. The basic line pattern of this chart is the same as that prescribed in the specification prepared by Commission I of the International Society of Photogrammetry in 1952 [1] which is listed under paragraph 1.3.3 of the specification as the "three line high contrast target." The three-line patterns reduce in size in a geometric progression, the ratio being $\sqrt[4]{2}$. The sizes of the patterns in the off-axis targets have been modified to compensate for the "cosine" and "cosine-squared" factors affecting the resolving power values for radial and tangential lines. For lenses having a focal length of 6 in., the range of values of resolving power in the image plane of the lens under test extends from 5.9 to 264 lines/mm.

c. Annulus Test Chart

At the time the chart containing the series of short three-line patterns was made, a series of annulus patterns was included as may be seen in figure 2. The range of sizes is the same as for the short three-line patterns. The shape of the off-axis patterns was also distorted so that at specified angles they register on the test negative as circles. This pattern differs from that described in the international specification in paragraph 1.3.5 [1] in that it is high-contrast and consists of a dark circle on a light background.

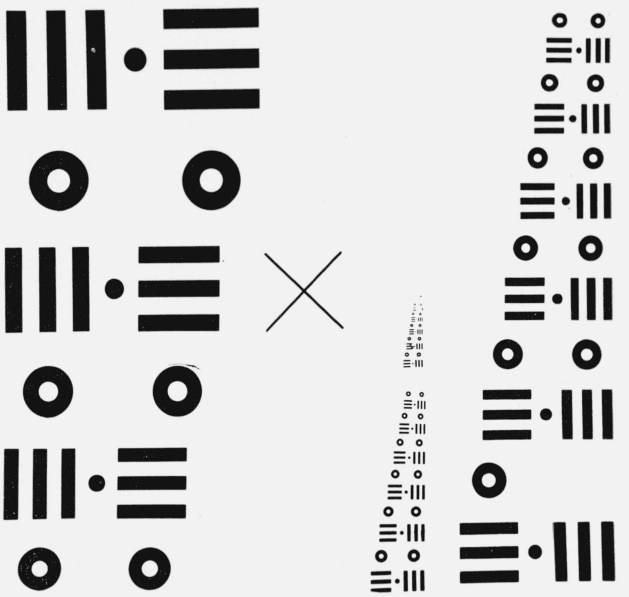

FIGURE 2. *Short three-line and annulus chart.*

The three-line chart consists of patterns of parallel lines in two orientations with spaces varying in a geometric progression by $\sqrt[4]{2}$. The circle or annulus charts change in size in a geometric progression by $\sqrt[4]{2}$. For a lens having a focal length of 6 in., the range of values in the image plane extends from 5.9 to 264 lines/mm.

2.3. Test Negative

In making the test negative, the lens under test is initially so alined that its optical axis is parallel to and approximately coincident with the axis of the collimated beam emergent from the first collimator. The lens is adjusted along the bench to a location such that the collimated beam at 40° from the axis fills the front aperture of the lens under test as viewed through the lens at an inclination of 40° from the axis. The plate holder is adjusted to a position such that the front surface of the emulsion is in the plane of best visual axial focus for the central row of images to be registered on the plate. The plate holder is then moved to a position 1.05 mm nearer to the lens, and an exposure is made by illuminating the reticles in odd-numbered collimators, which thus registers the imagery on the plate at 10° intervals for the range of angles from $\beta=0$ to $\beta=40°$. This process is repeated with the plate being moved 0.15 mm farther from the lens until 15 exposures have been made with the last for the plane 1.05 mm farther from the lens than the position of best visual axial focus. Between each exposure, the plate holder is also moved downward by an amount sufficient to avoid superposition of successive rows of images. The foregoing operation registers the imagery for the long-line patterns on the plate. The plate holder is then returned to its initial position for which the emulsion surface is 1.05 mm nearer to the lens than the plane of best visual axial focus; the plate is displaced sidewise in its holder approximately 12 mm; and the entire bench on which the camera is mounted is rotated on its pivot by 5° so

that the axis of the lens is now parallel to and nearly coincident with the axis of the collimated beam emergent from the second collimator. The foregoing procedure is then repeated with the exception that exposures are made by illuminating the reticles in the even-numbered collimators, which again register imagery on the plate at 10° intervals for the range of angles from $\beta=0°$ to $\beta=40°$. This process registers the imagery for the short three-line and annulus patterns on the plate. The exposed plate is then processed to form the finished negative from which values of resolving power are determined.

All exposures are made with the reticles illuminated by light from tungsten lamps with K–3 filters between the light source and test charts. Neutral filters are used to adjust the intensity of the illumination of the plate so that the final resulting optical density of each image on the negative is approximately the same for all values of β. The two types of photographic plates used in this work were Eastman Spectroscopic VF, which has a fine-grained panchromatic emulsion, and Eastman Super Panchro Press, Type C.

2.4. Reading the Negative

The negative images were examined with a microscope using powers ranging from 30× to 50×. The criteria for declaring a particular line pattern to be the finest resolved were that all coarser patterns were clearly resolved and that the number of lines in a given pattern was the same as that of the corresponding pattern in the object. For the annulus pattern, the prime criterion that all coarser patterns were resolved was used.

It was readily apparent that there were marked differences in the ease of reading the three types of patterns. The long-line pattern was the easiest of the three, and the feeling of confidence in the values recorded was accordingly the greatest. The short-line pattern was the next easiest, but there was an appreciably higher level of uncertainty in the reliability of the higher values of resolving power. The annulus pattern was the most difficult when attempting to determine the limit of resolution. It is noteworthy that the single circular black spot, which appears on the test chart in each cell of the target and which is identical in size with the white inner circular area of the annulus pattern, was easier to read than the annulus. It was usually possible to distinguish this single spot on the negative down to smaller sizes than the annulus; it could usually be detected down to one or two steps smaller in size. The presence of this spot was frequently used as an aid in determining the limiting resolution for the annulus.

3. Results of Measurements

The results of measurement on six wide-angle lenses are reported and analyzed in this study. Three lenses, designated Nos. 1, 2, and 5, are essentially distortion free; the other three, designated 3, 4, and 6, have moderate amounts of distortion. Measurements of resolving power were made at 10° intervals from 0° to 40°.

Negatives were made with both VF and SP emulsions for each of the six lenses. For a given lens, the plane of best visual axial focus is the same for each emulsion. The measured equivalent focal length for the plane of best visual axial focus for a given lens was the same for each emulsion and type of target pattern. The maximum range of change in measured equivalent focal length for the various conditions of test did not exceed ± 0.02 mm for a given lens.

In the presentation and analysis of the results of measurement in an investigation of this sort, it is necessary to keep in mind the primary aims of the study. First, the intercomparison of the magnitudes of the measured values of resolving power for each type of pattern and emulsion is important. Second, it is important to determine whether or not any shift of the plane of best definition occurs with type of target pattern. In addition, the manner in which the values of resolving power for the various patterns wax and wane as the image plane approaches and passes through the plane of best visual axial focus is of interest.

In an earlier paper [10], the measured values of resolving power for tangential lines (T_β) and radial lines (R_β) obtained with the short three-line chart using VF and SP emulsions for values of β ranging from 0° to 40° at 10° intervals are presented in tabular form for lens No. 1. In addition, the values of the geometric means values $\sqrt{R_\beta T_\beta}$ are also given. In this paper, a discussion of the various indices used in locating the plane of best average definition is given. These indices are as follows:

(*a*) *Root Mean Square Mean* (*RMSM*). This is defined as

$$\text{RMSM}=\sqrt{\frac{\sum R_\beta T_\beta}{n}}=\sqrt{\overline{R_\beta T_\beta}}.$$

In the above expression, R_β and T_β are measured values of resolving power for radial and tangential lines for discrete values of β ranging from 0° to 40° in 10° steps. The number of steps, n, in this instance is five.

(*b*) *Area Weighted Average Resolution* (*AWAR*). This is defined as

$$\text{AWAR}=\sum \frac{a_\beta}{A}\sqrt{R_\beta T_\beta},$$

where a_β is the area of a particular annular zone, R_β is the average resolving power for radial lines, and T_β is the average resolving power for tangential lines for that zone. The value of $\sum a_\beta$ is the entire area A of the picture formed.

(*c*) *Area and Depth-of-Focus Weighted Average Resolution* (*ADWAR*). This is defined as

$$\text{ADWAR}=\sum \frac{a_\beta r_\beta}{A}\sqrt{R_\beta T_\beta},$$

where

$$r_\beta^2 = \frac{d_0 d_0}{d_{T_\beta} d_{R_\beta}},$$

where d_{T_β} is the depth of focus for tangential lines, d_{R_β} is the depth of focus for radial lines, and d_0 is the depth of focus on axis for a given value of resolving power.

Because some of the results for one type of pattern used in this paper have already been presented in tabular form, it was decided to present the results of measurement and some of the quantities derived from the measurements in graphical form.

The results of measurement are presented in figures 3 through 9. Values of the resolving power for tangential lines (T) and radial lines (R) are shown for the two emulsions and three patterns for lenses 1 and 3 only. These results on these two lenses are given in the left and central columns of graphs in figures 3, 4, 5, and 6. The nature of the test pattern is indicated by the symbols, L for long-line, S for short-line, and A for annulus. The values obtained for the annular patterns are shown on both sets of graphs for ready comparison with the T and R values for L and S. It is readily apparent from these graphs that the higher values found for resolution of long lines are more evident for the regions inside focus (negative values of Δf) than for the regions outside focus (positive values of Δf). This is in keeping with a similar finding reported by Selwyn and Tearle [11]. This effect is present for both VF and SP emulsions for axial resloving power; it is usually more noticeable for the VF emulsion. The values found for the annulus pattern are generally substantially lower than the values for either tangential or radial lines throughout the region of usable imagery as might be inferred from similar comparisons previously reported [5, 6].

The values of $\sqrt{R_\beta T_\beta}$, the geometric mean value of resolving power for tangential and radial lines, are given for each value of β for each of the six lenses for both emulsions. For lenses No. 1 and 3, values of $\sqrt{R_\beta T_\beta}$ are shown in the right-hand column of figures 3, 4, 5, and 6. The values of $\sqrt{R_\beta T_\beta}$ for lenses No. 2, 5, 4, and 6 are presented in the five upper sets of graphs in figures 8 and 9. These curves permit a ready comparison of the average values of resolving power for the three types of patterns for the five values of β. It also seems more appropriate to use values of $\sqrt{R_\beta T_\beta}$ in a comparison of values obtained by line targets with that obtained by the annulus target. For the annulus, the value of $\sqrt{R_\beta T_\beta}$ is simply the observed value of the resolving power.

For lenses No. 1 and 3, values of the three indices $\sqrt{R_\beta T_\beta}$, AWAR, and ADWAR for the three types of line patterns and two emulsions are given in figure 7. For lenses 2, 5, 4, and 6, values of $\sqrt{R_\beta T_\beta}$ are shown in the lower row of graphs in figures 8 and 9. Values of AWAR and ADWAR were determined for these four lenses but are not shown.

3.1. Location of the Plane of Best Average Definition

The plane of best average definition was located for each lens both by graphical analysis and by location of the maximum value of the various indices for each type of pattern and each emulsion.

a. Graphical Analysis

The plane of best average definition for each lens for each set of conditions was located by the graphical method reported in a previous paper [10]. The separations, Δf, along the optical axis of the lens of the focal planes of best average definition for short-line and annular patterns selected by graphical analysis from the focal planes of best average definition for long-line patterns selected in the same manner, are shown in table 1. It is clear from this table that there is no significant variation in the location of the focal plane of best average definition for these three types of test pattern. Such variation, as appears is usually random and within the limits of experimental error. Table 2 shows the variation in location of the plane of best average definition for the three types of patterns using SP emulsion compared with that for long-line patterns and VF emulsion. In this instance, the optimum image plane for SP emulsion appears on the average to be slightly nearer the lens than the corresponding plane for VF emulsion.

TABLE 1. *Separations, Δf, of the focal plane of best average definition for long lines selected by graphical analysis from focal planes of best average definition for short-line and annulus patterns selected by graphical analyses*

Results are given for six lenses and two emulsions.

Lens No.	Values of Δf			
	VF emulsion		SP emulsion	
	Short line	Annulus	Short line	Annulus
	mm	*mm*	*mm*	*mm*
1	0.00	0.15	0.00	0.00
2	.00	.15	.00	−.15
3	.30	.00	.00	.00
4	.00	.15	.00	.00
5	.00	.00	.00	.00
6	.00	.00	.00	.00

TABLE 2. *Separations, Δf, of the focal plane of best average definition for long lines with VF emulsion selected by graphical analysis from the focal planes of best average definition for long line, short line, and annulus patterns obtained with SP emulsion by graphical analyses*

Lens No.	Values of Δf		
	Long line	Short line	Annulus
	mm	*mm*	*mm*
1	0.15	−0.15	−0.15
2	−.15	−.15	−.30
3	.00	.00	.00
4	.00	.00	.00
5	.00	.00	.00
6	−.15	−.15	−.15

549993—60——4

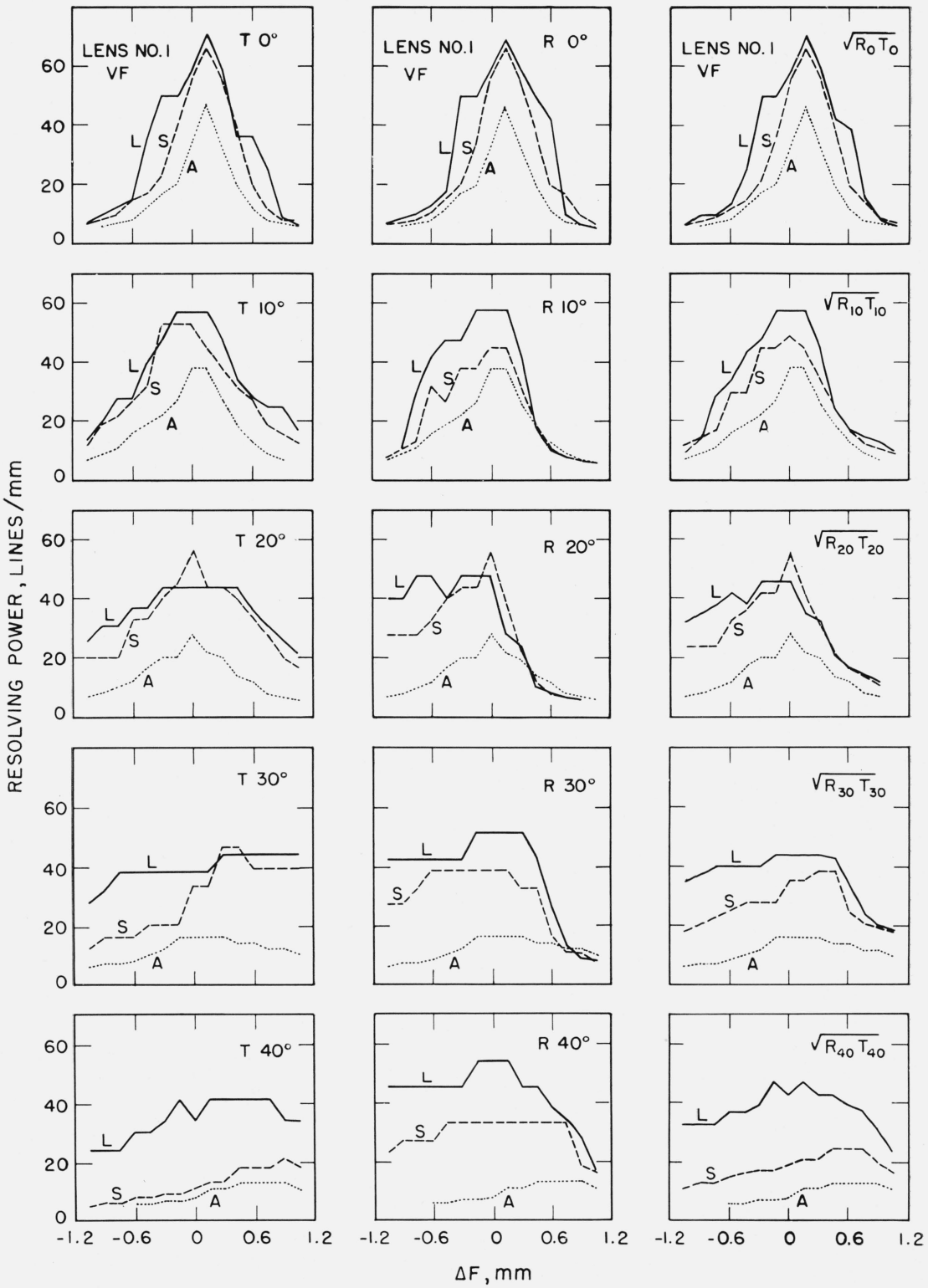

FIGURE 3. *Resolving power versus position of the image plane for lens No. 1 with VF emulsion.*

The resolving power throughout the region of usable imagery is shown for tangential (T) and radial (R) lines and for the average $\sqrt{R_\beta T_\beta}$ at 10° intervals from 0° to 40°. Values are given for long-line (L) and short-line (S) test patterns. Values for the annular (A) pattern are shown with the corresponding T, R, and $\sqrt{R_\beta T_\beta}$ values for ready comparison. The zero of abscissas (Δf) marks the position of best visual axial focus, and positive values of abscissas indicate positions farther from the lens.

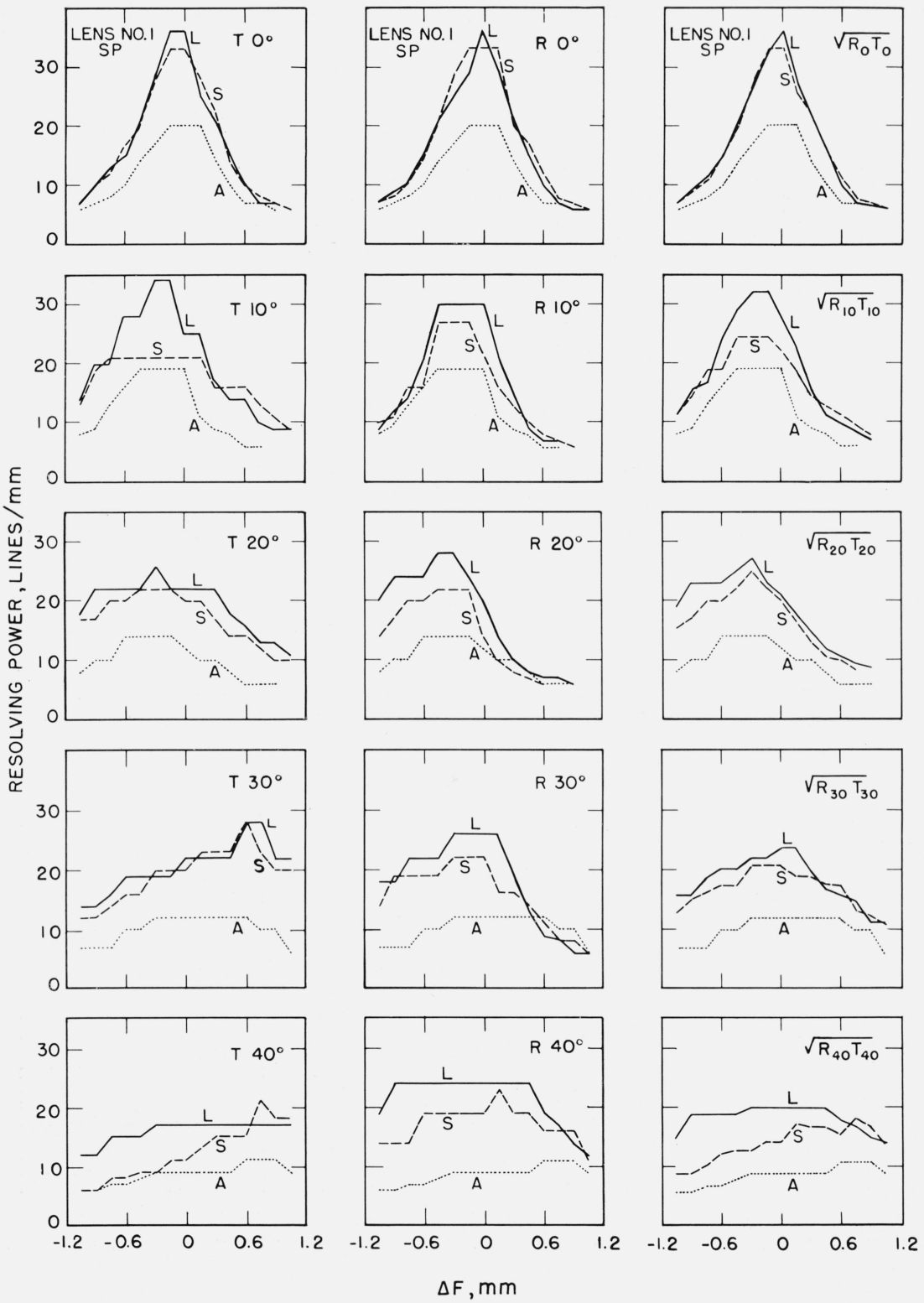

FIGURE 4. *Resolving power versus position of the image plane for lens No. 1 with SP emulsion.*

The resolving power throughout the region of usable imagery is shown for tangential (T) and radial (R) lines and for the average $\sqrt{R_\beta T_\beta}$ at 10° intervals from 0° to 40°. Values are given for long-line (L) and short-line (S) test patterns. Values for the annular (A) pattern are shown with the corresponding T, R, and $\sqrt{R_\beta T_\beta}$ values for ready comparison. The zero of abscissas (Δf) marks the position of best visual axial focus, and positive values of abscissas indicate positions farther from the lens.

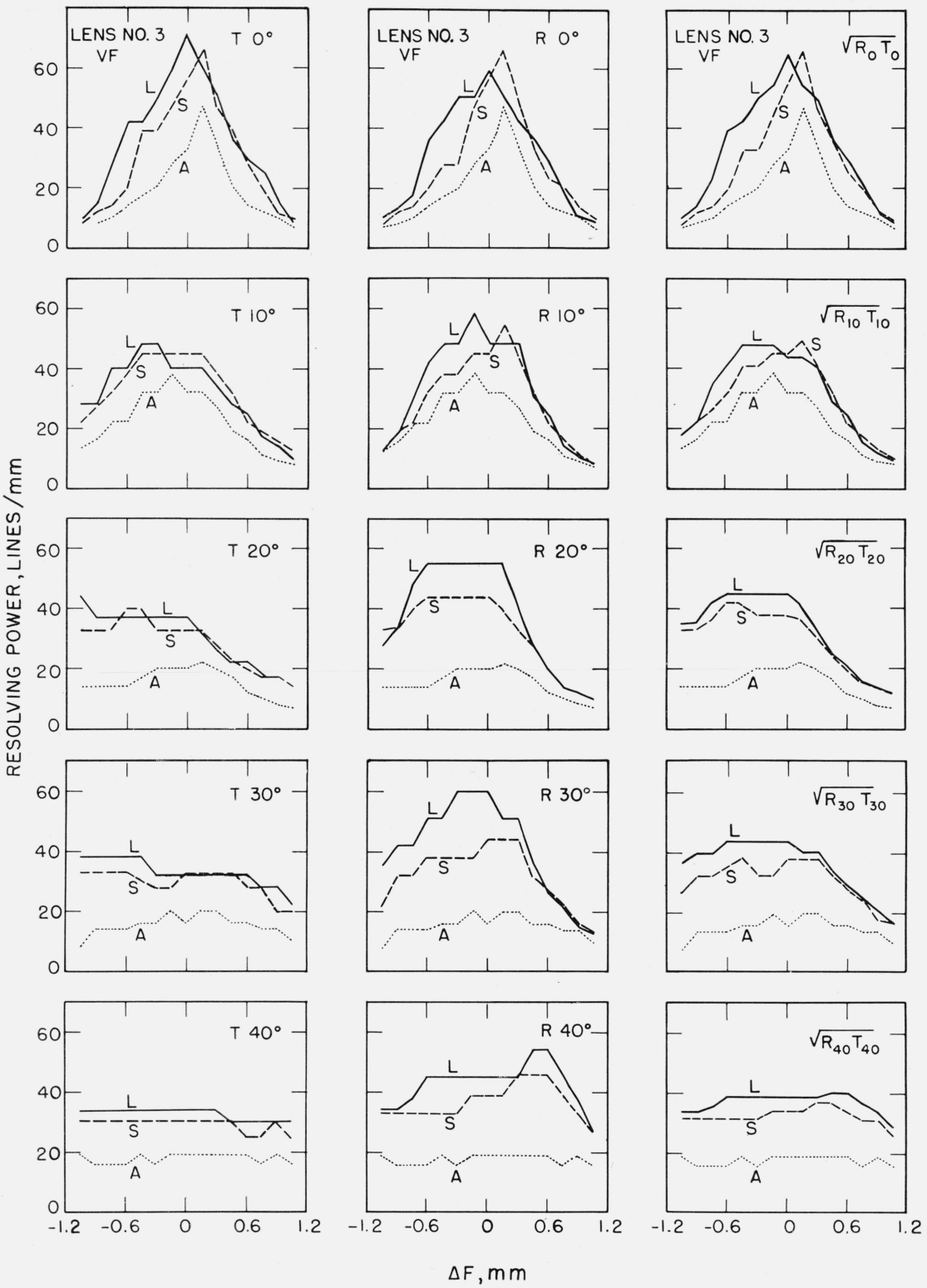

FIGURE 5. *Resolving power versus position of the image plane for lens No. 3 with VF emulsion.*

This set of curves gives information on lens No. 3 of the same type that is given in figure 3 for lens No. 1.

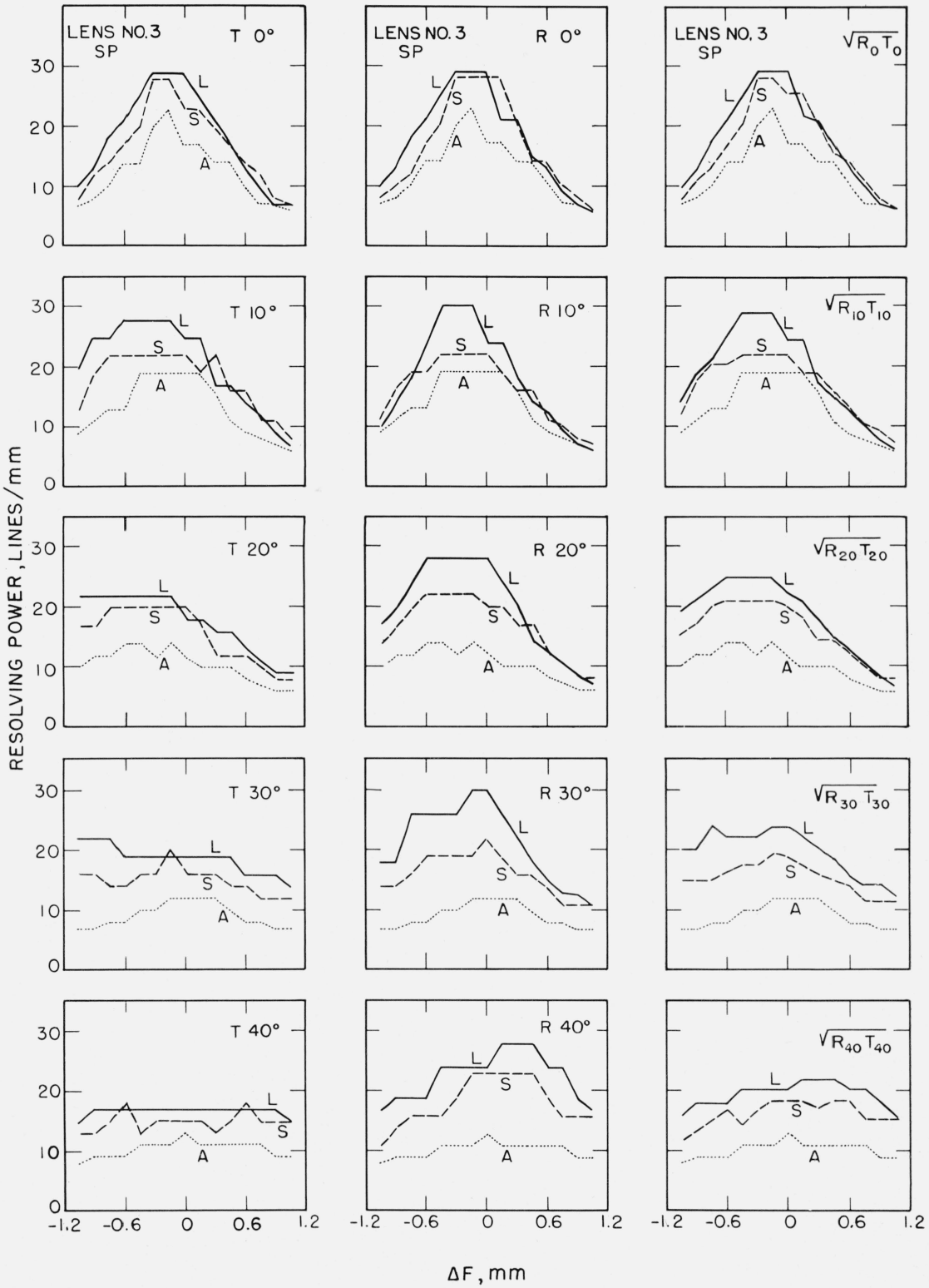

FIGURE 6. *Resolving power versus position of the image plane for lens No. 3 with SP emulsion.*

This set of curves gives information on lens No. 3 of the same type that is given in figure 4 for lens No. 1.

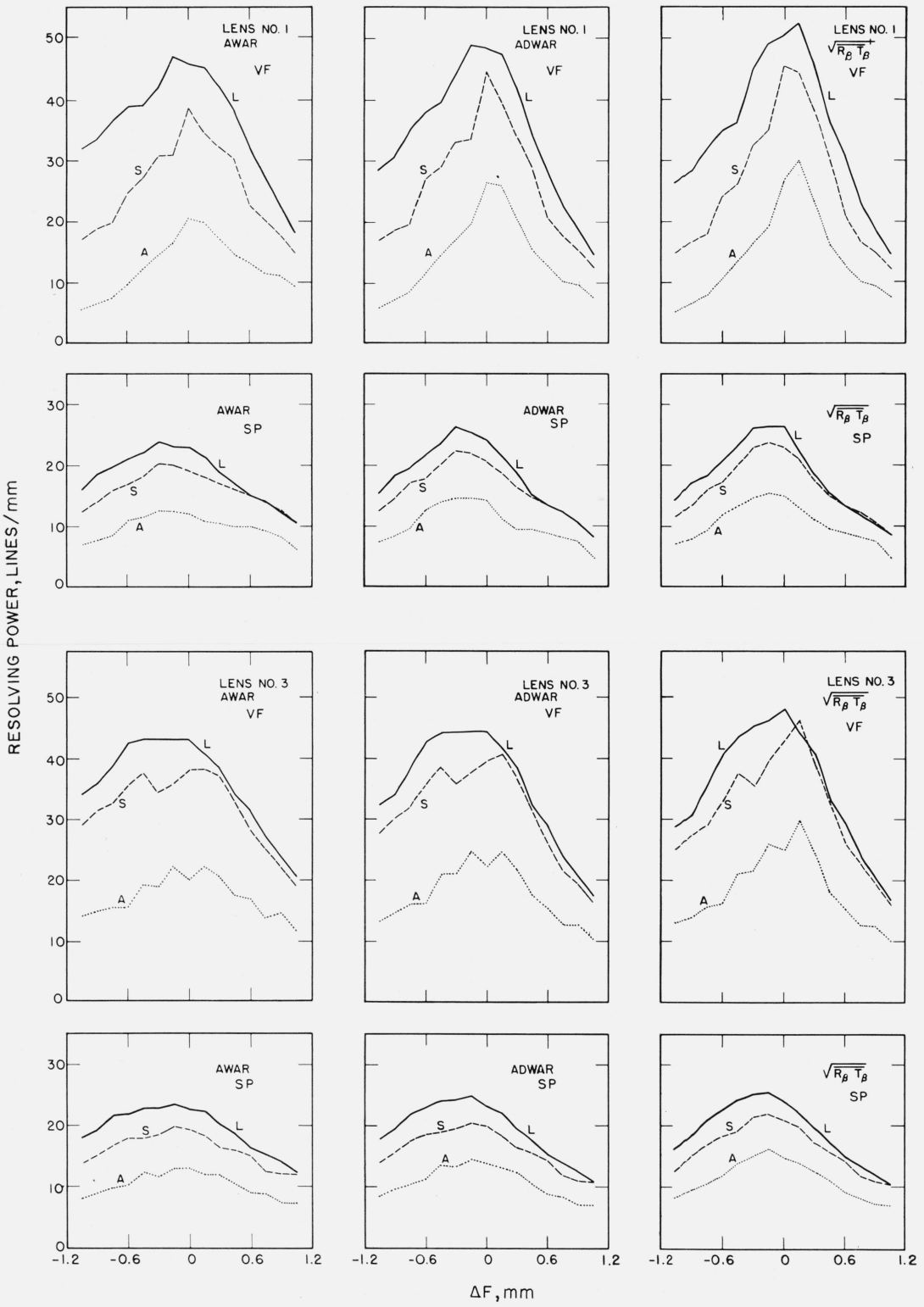

FIGURE 7. *Variation of AWAR, ADWAR, and* $\sqrt{R_\beta T_\beta}$ *with position of the image plane for lenses Nos. 1 and 3 for VF and SP emulsions.*

Values of these indices are given in lines per millimeter for long-line (*L*), short-line (*S*), and annular (*A*) patterns. The zero of abscissas (Δf) marks the position of best visual axial focus, and positive value of abscissas indicate positions farther from the lens.

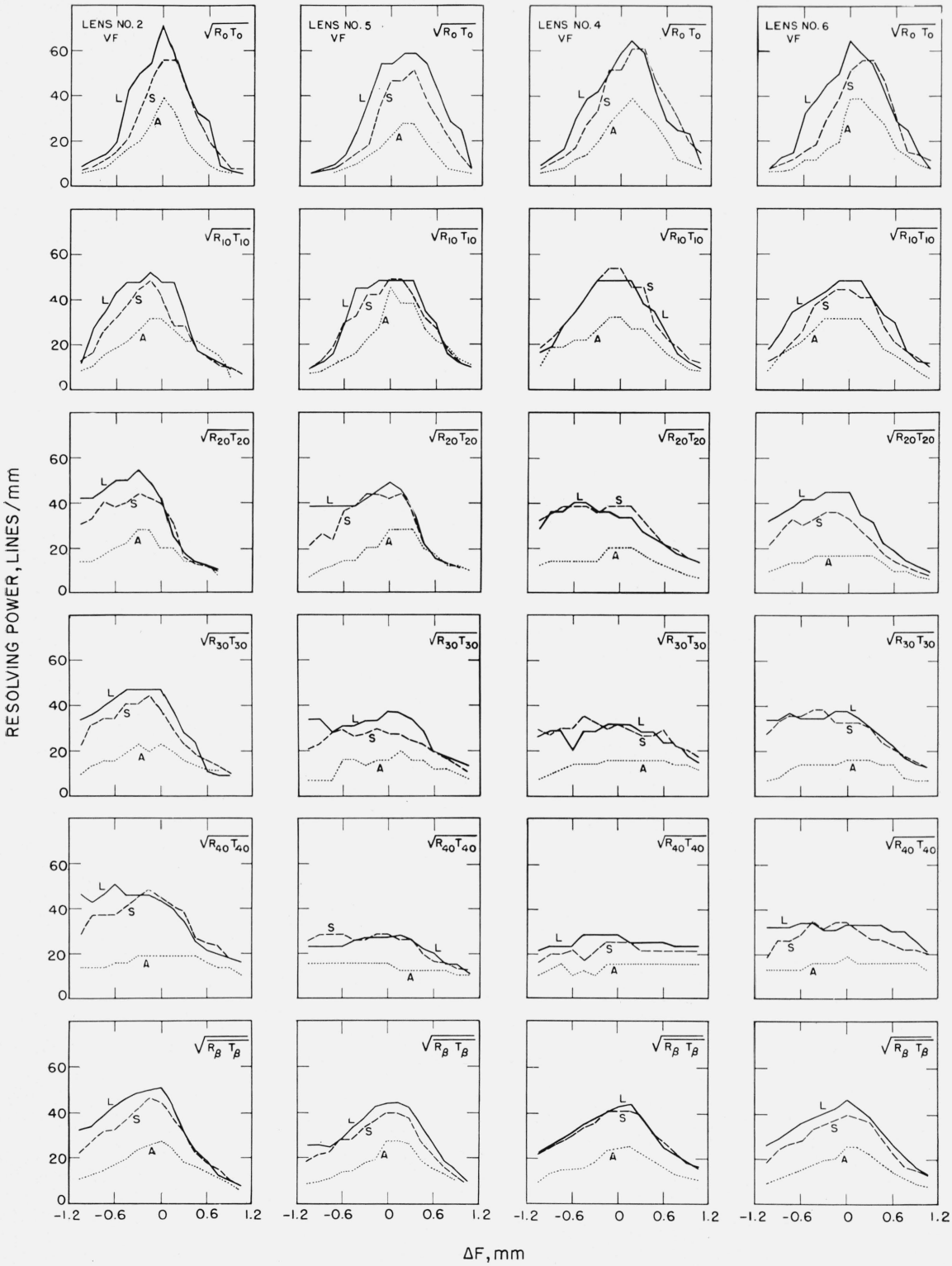

FIGURE 8. *Average resolving powers versus position of the image plane for four lenses with VF emulsions.*

Values of the average resolving power $\sqrt{R_\beta T_\beta}$ are shown at 10° intervals from 0° to 40°. The lowest box in each column shows values of the root mean square mean $\sqrt{\overline{R_\beta T_\beta}}$. Values are given for long-line (*L*), short-line (*S*), and annular (*A*) patterns. The zero of abscissas (Δf) marks the position of best visual axial focus, and positive value indicate positions farther from the lens.

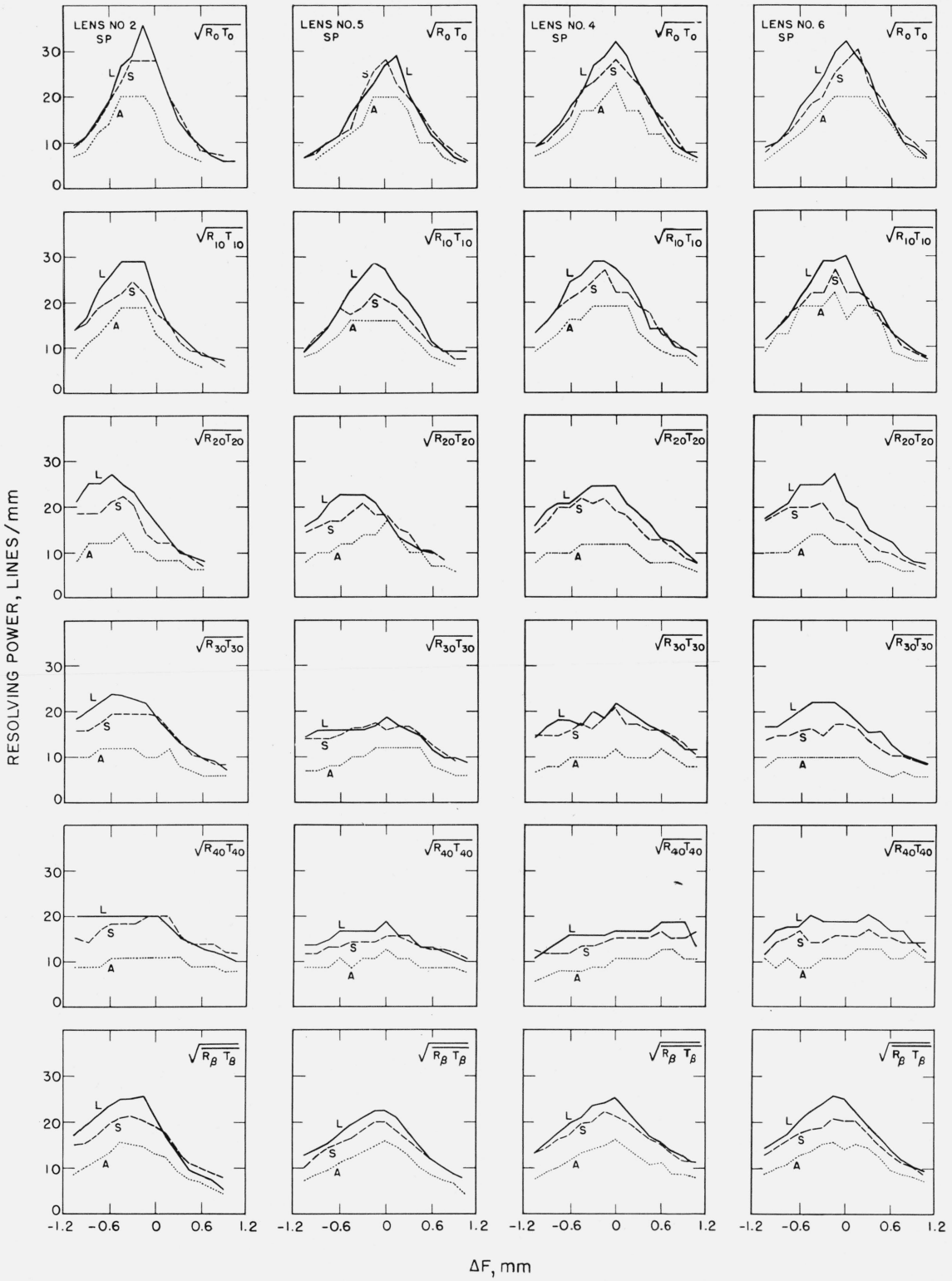

FIGURE 9. *Average resolving powers versus position of the image plane for four lenses with SP emulsions.*

Values of the average resolving power $\sqrt{R_\beta T_\beta}$ are shown at 10° intervals from 0° to 40°. The lowest box in each column shows values of $\sqrt{\overline{R_\beta T_\beta}}$. Values are given for long-line (*L*), short-line (*S*), and annular (*A*) patterns. The zero of abscissas marks the position of best visual axial focus, and positive value indicate positions farther from the lens.

b. Maximum Value of Indices

The plane of best average definition for each lens for each set of conditions was also located with the aid of each of the three indices, $\sqrt{\overline{R_\beta T_\beta}}$, AWAR, and ADWAR. In each instance, the optimum image plane was located with respect to the focal plane of best average definition for long-line patterns selected by graphical analysis. The results are shown in table 3. It is clear from this table that the variation is, in general, within the limits of experimental error.

TABLE 3. *Separations, Δf, of the focal plane of best average definition for long lines selected by graphical analysis from the focal planes indicated by the maximum value of the indices* $\sqrt{\overline{R_\beta T_\beta}}$, *AWAR, and ADWAR*

Results are shown for six lenses and two emulsions.

Lens No.	VF emulsion			SP emulsion		
	Long line	Short line	Annulus	Long line	Short line	Annulus
(a) Separations, Δf, of plane selected by graphical analysis from planes selected by maximum value of $\sqrt{\overline{R_\beta T_\beta}}$ for						
	mm	*mm*	*mm*	*mm*	*mm*	*mm*
1	0.15	0.00	0.15	0.00	0.00	0.00
2	.15	.00	.15	.15	.00	−.15
3	.15	.30	.30	.00	.00	.00
4	.15	.00	.15	.00	−.15	.00
5	.15	.15	.00	.00	.00	.00
6	.00	.00	.00	.00	.00	.00
(b) Separations, Δf, of plane selected by graphical analysis from planes selected by maximum value of AWAR for						
1	−0.15	0.00	0.00	−0.15	−0.15	0.00
2	−.15	.00	−.15	−.30	−.15	−.15
3	−.30	.30	.00	.00	.00	.15
4	.00	.00	−.15	.00	.00	.00
5	.00	.00	.00	.00	−.15	.00
6	.00	−.30	.00	.00	.00	.00
(c) Separations, Δf, of plane selected by graphical analysis from planes selected by maximum value of ADWAR for						
1	−0.15	0.00	0.00	−0.15	−0.15	0.00
2	.00	.00	.00	−.15	.00	−.15
3	−.15	.30	.00	.00	.00	.00
4	.00	−.15	−.15	.00	−.15	.00
5	.00	.00	.00	.00	−.15	.00
6	.00	−.15	.00	.00	.00	.00

4. Comparison of Results Obtained With the Three Charts

In the foregoing sections, it was shown that the focal plane of best average definition could be readily located using any one of the three types of test charts under consideration. Moreover, such minor differences in location that were noted could be regarded as negligible in comparison with experimental error.

In the present section, some attention is given to the actual magnitudes of the values of resolving power obtained with the various charts. Some attention is also given to the use of the indices as rating factors.

4.1. Values of Resolving Power in Focal Plane of Best Average Definition

Values of $\sqrt{R_\beta T_\beta}$, $\sqrt{\overline{R_\beta T_\beta}}$, AWAR, and ADWAR are shown in tables 4 and 5 for various patterns and emulsions. These values are all for the plane of best average definition for long-line patterns. In some instances, the value of a given index was higher for an adjacent plane. This is indicated in table 6 which shows the departure in percent of the maximum of a given index from the value reported in tables 4 and 5. It is noteworthy that the departures are for the most part negligible. It is clear from tables 4 and 5 that it would be difficult to determine the value of resolving power that might be obtained for a given type of pattern at a given angle β when

TABLE 4. *Comparison of values of average resolving power obtained with three types of test chart using VF emulsion in the plane of best average definition for long lines selected by graphical analysis.*

Values of $\sqrt{R_\beta T_\beta}$, $\sqrt{\overline{R_\beta T_\beta}}$, AWAR, and ADWAR are shown for six lenses for long line, short line, and annulus charts. All values of resolving power are given in lines per millimeter.

Lens No.	Target	$\sqrt{R_\beta T_\beta}$					Indices		
		0°	10°	20°	30°	40°	$\sqrt{\overline{R_\beta T_\beta}}$	AWAR	ADWAR
1	Long line	59	58	46	44	43	50	46	49
	Short line	56	49	56	35	19	45	38	45
	Annulus	33	38	28	16	8	27	20	26
2	Long line	54	52	49	47	46	50	48	49
	Short line	47	49	42	45	49	46	46	46
	Annulus	28	32	28	20	19	26	23	26
3	Long line	54	48	45	44	39	46	43	46
	Short line	66	49	36	38	34	46	38	41
	Annulus	33	32	20	16	19	25	20	22
4	Long line	59	48	39	32	29	43	35	38
	Short line	51	54	34	33	26	41	34	38
	Annulus	33	32	20	16	13	24	18	21
5	Long line	54	48	49	38	28	44	39	41
	Short line	47	49	42	28	29	40	34	38
	Annulus	23	45	28	16	16	28	23	28
6	Long line	65	48	45	38	33	47	39	42
	Short line	51	45	34	33	34	40	35	37
	Annulus	39	32	17	16	19	26	20	22

TABLE 5. *Comparison of values of average resolving power obtained with three types of test chart using SP emulsion in the plane of best average definition for long lines as selected by graphical analysis*

Values of $\sqrt{R_\beta T_\beta}$, $\sqrt{\overline{R_\beta T_\beta}}$, AWAR, and ADWAR are shown for six lenses for long line, short line, and annulus charts. All values of resolving power are given in lines per millimeter.

Lens No.	Target	$\sqrt{R_\beta T_\beta}$					Indices		
		0°	10°	20°	30°	40°	$\sqrt{\overline{R_\beta T_\beta}}$	AWAR	ADWAR
1	Long line	32	32	23	22	20	23	25	26
	Short line	33	24	22	21	14	24	20	22
	Annulus	20	19	14	13	9	15	12	15
2	Long line	29	29	23	23	20	25	23	25
	Short line	25	24	20	20	18	22	20	21
	Annulus	20	19	10	12	11	15	12	14
3	Long line	29	29	25	24	20	26	24	25
	Short line	28	22	21	20	19	22	20	21
	Annulus	23	19	14	12	11	16	13	14
4	Long line	32	27	25	22	17	25	22	24
	Short line	25	27	22	19	14	22	19	21
	Annulus	23	19	12	12	11	16	13	14
5	Long line	27	27	21	19	19	23	20	22
	Short line	28	20	18	16	16	20	17	18
	Annulus	20	16	17	12	13	16	14	15
6	Long line	30	29	27	22	19	23	25	26
	Short line	25	27	18	18	16	21	18	20
	Annulus	20	22	12	10	11	16	12	14

TABLE 6. *Departure in percent of the maximum value of a given index from that occurring in the plane of best average definition for long lines selected by graphical analysis*

Results are shown for $\sqrt{R_\beta T_\beta}$, AWAR, and ADWAR for six lenses with each type of target for VF and SP emulsions.

Lens No.	VF			SP		
	$\sqrt{R_\beta T_\beta}$	AWAR	ADWAR	$\sqrt{R_\beta T_\beta}$	AWAR	ADWAR
	Long-line			Long-line		
1	4.0	2.6	0.6	3.4	3.0	0.0
2	2.5	1.0	.0	2.7	1.7	1.6
3	3.3	0.0	3.3	0.0	0.0	0.0
4	3.0	.0	0.0	.0	.0	.0
5	0.9	.0	.0	.0	.0	.0
6	.0	.0	.0	.0	.0	.0
	Short-line			Short-line		
1	0.0	0.0	0.0	0.0	1.5	1.8
2	.0	.0	.0	.0	1.0	0.0
3	.0	.0	.0	.0	0.0	.0
4	.0	.0	.2	.0	.5	.0
5	.5	.0	.0	.0	1.2	1.6
6	.0	3.6	.5	.0	0.0	0.0
	Annulus			Annulus		
1	0.0	3.9	1.9	0.0	0.0	0.0
2	6.5	0.0	0.0	3.8	6.1	6.7
3	13.0	.0	.0	0.0	0.8	0.0
4	3.6	.5	.5	.0	.0	.0
5	0.0	.0	.0	.0	.0	.0
6	.0	.0	.0	.0	.0	.0

the value of resolving power for a different type pattern is known. The relative magnitudes of $\sqrt{R_\beta T_\beta}$ at a given value of β for the various type patterns are significantly different for the different lenses. Certain generalizations can, however, be drawn. The values of $\sqrt{R_\beta T_\beta}$ in general are highest for the long-line and lowest for the annular patterns with the values for the short-line patterns being usually slightly lower than those for the long-line patterns.

4.2. Use of Indices as Rating Factor

In table 7, the relative ratings of lenses 1 through 6 are shown for each of the various conditions of test. It is, at once, apparent that the order of merit is not the same for the various patterns. This variation in the order of merit emphasizes the fact that indices such as these ought not to be used to differentiate between lenses unless the differences are of the order of 10 percent or more. Thus, in considering the relative merits of these lenses, 1, 2, and 3 are usually more favorably rated than 4, 5, and 6. However, it would be difficult to arrange 1, 2, and 3 in order of decreasing performance. Likewise, it would be difficult to arrange 4, 5, and 6 in proper order. Most of this difficulty arises from the relatively small differences in the particular index.

4.3. Relative Magnitudes of Values of Resolving Power

a. For Three Types of Test Pattern

It was evident at a fairly early stage in the investigation that there is no clear-cut ratio existing between

TABLE 7. *Rating of six lenses in order of merit for VF and SP emulsions*

The ratings are made for each of three targets on the basis of the relative magnitude of the three indices $\sqrt{R_\beta T_\beta}$, AWAR, and ADWAR.

Lens No.	VF emulsion			SP emulsion		
	Rating based on			Rating based on		
	$\sqrt{R_\beta T_\beta}$	AWAR	ADWAR	$\sqrt{R_\beta T_\beta}$	AWAR	ADWAR
	(a) Long-line			(a) Long-line		
1	1	2	1	4	1	1
2	1	1	1	2	4	3
3	4	3	3	1	3	3
4	6	6	6	2	5	5
5	5	4	5	4	6	6
6	3	4	4	4	1	1
	(b) Short-line			(b) Short-line		
1	3	2	2	1	1	1
2	1	1	1	2	1	2
3	1	2	3	2	1	2
4	4	5	4	2	4	2
5	5	5	4	6	6	6
6	5	4	6	5	5	5
	(c) Annulus			(c) Annulus		
1	2	3	2	5	4	1
2	3	1	2	5	4	3
3	5	3	4	1	2	3
4	6	6	6	1	2	3
5	1	1	1	1	1	1
6	3	3	4	1	4	3

values of resolving power obtained for one type of pattern and those obtained for another type of pattern. This is at once apparent from consideration of the various curves in figures 3 through 9. Even on axis, there are variations which might be in part a consequence of the large interval between successive patterns but are more likely a consequence of the inherent uncertainty in locating the limit of resolution. However, some idea of the approximate magnitude of the values of resolving power for the various patterns relative to one another can be gained from consideration of the relative magnitudes of the various indices. Ratios have been computed for long-line versus short-line, short-line versus annulus, and long-line versus annulus for the various indices for VF and SP emulsions. These ratios are shown in table 8. From these values, one may infer that the values of resolving power obtained with long-line patterns using SP emulsion are likely to be 18 percent higher than values obtained with short-line patterns. In a similar manner, values for short-line patterns may be expected to be 45 percent higher than for annular patterns. Long-line patterns may be expected to yield values approximately 70 percent higher than annular patterns.

b. For Two Types of Emulsion

Of the two emulsions for which values are reported in this study, the VF emulsion has been used at the Bureau over a long period of years in making the negatives used in evaluating equivalent focal length, distortion, and resolving power of lenses. It has been eminently satisfactory for this purpose, and

TABLE 8. *Ratio of values of given indices as a function of pattern type*

Values are given (a) for the average ratio (L/S) of the values of a given index for long lines and the same index for short lines. Values are also given (b) of the average ratio (S/A) of the values of a given index for short lines and the same index for annulus type patterns. Values are also shown of the average ratio (L/A) of the values of a given index for long lines and the same index for annulus type patterns. Values are shown for both VF and SP emulsions together with the probable error of a single observation (PE_s) for each ratio.

Index	(a) Values of L/S and PE_s for emulsion			
	VF		SP	
	L/S	PE_s	L/S	PE_s
$\overline{R_\beta T_\beta}$	1.09	±0.04	1.11	±0.05
AWAR	1.11	.05	1.22	.06
ADWAR	1.08	.03	1.20	.03
	(b) Values of S/A and PE_s for emulsion			
	S/A	PE_s	S/A	PE_s
$\sqrt{\overline{R_\beta T_\beta}}$	1.66	±0.11	1.40	±0.09
AWAR	1.82	.12	1.51	.11
ADWAR	1.70	.11	1.43	.07
	(c) Values of L/A and PE_s for emulsion			
	L/A	PE_s	L/A	PE_s
$\overline{R_\beta T_\beta}$	1.80	±0.07	1.55	±0.07
WAR	2.02	.14	1.84	.18
DWAR	1.84	.12	1.72	.08

numerous specifications involving resolving power of lenses are based upon determinations made therewith. In recent years, there has been a tendency on the part of many engaged in evaluating lens performance to use emulsions similar to the SP emulsion used in this study. This practice is justified on the grounds that with this emulsion, the test conditions more nearly approximate the conditions of use.

Because the two types of emulsion are used for much the same purpose, it is of interest to compare the values of resolving power under like conditions for the two emulsions. It is clear from the curves shown in figures 3 through 9, that there is no clear-cut ratio that is valid for all conditions of focus and for all angular separations from the axis. Accordingly, the ratios existing between the values of the various indices for the two emulsions were determined and are shown in table 9. From this table, one may infer that the values of resolving power obtained with VF emulsion are likely to be 84 percent higher for long-line patterns, 98 percent higher for short-line patterns, and 66 percent higher for annular patterns than are obtained for SP emulsion.

TABLE 9. *Ratio* q *of the value of a given index in plane of best average definition for VF emulsion to the value of the same index in the plane of best average definition for SP emulsion for three types of test patterns*

Values of the ratio are shown $\sqrt{\overline{R_\beta T_\beta}}$, AWAR, and ADWAR obtained with long-line, short-line, and annular patterns. These are average values for six lenses, and the probable error of a single determination of each ratio is also shown.

Index	Ratio for patterns comprised of					
	Long lines		Short lines		Annuli	
	q	PE_s	q	PE_s	q	PE_s
$\sqrt{\overline{R_\beta T_\beta}}$	1.94	±0.12	1.97	±0.09	1.66	±0.09
AWAR	1.80	.14	1.97	.11	1.64	.11
ADWAR	1.79	.11	1.99	.11	1.68	.13

5. Conclusion

In this study, the values of the resolving power of six lenses were measured using three types of target pattern and two emulsions. Analysis of the results of measurements leads to the following conclusions.

(1) For either of the two emulsions used, the same plane of best average definition is usually selected by graphical analysis for long-line, short-line, and annulus target patterns.

(2) The plane of best average definition located with the VF emulsion is generally identical with that located with SP emulsion.

(3) While small variations in the location of the focal plane occur with type of index used, these variations are generally sufficiently small that the plane selected by anyone of the three indices is likely to prove satisfactory.

The authors express their appreciation to other members of the staff of the National Bureau of Standards for assistance during this work and in particular to E. C. Watts who prepared the illustrations.

6. References

[1] Rept. of Comm. I, Intern. Soc. Photogrammetry, Specification of methods of calibrating photogrammetric cameras and measuring their resolution, image illumination, and veiling glare, Photogrammetria **X,** 85 (1953–1954).

[2] Military Standard MIL–STD–150–A; Photographic lenses.

[3] British Standard 1613 : 1949, Resolving power of lenses for cameras and enlargers.

[4] L. E. Howlett, Photographic resolving power, Can. J. Research **24** [A], 15–40 (1946).

[5] F. H. Perrin and J. H. Altman, Studies in the resolving power of photographic emulsions, VI. The effect of the type of test pattern and luminance ratio in the test object, J. Opt. Soc. Am. **43,** 780 (1953).

[6] P. Hariharan, Resolving power of photographic emulsions **46,** 315 (1956).

[7] F. E. Washer and I. C. Gardner, Method for determining the resolving power of photographic lenses, NBS Circ. 533 (1953).

[8] I. C. Gardner and F. A. Case, Precision camera for testing lenses, J. Research NBS **18,** 449 (1937) RP984.

[9] F. E. Washer and F. A. Case, Calibration of precision airplane mapping cameras, J. Research NBS **45,** 1 (1950) RP2108; Photogrammetric Eng. **XVI,** 502 (1950).

[10] F. E. Washer and W. P. Tayman, Location of the plane of best average definition for airplane camera lenses, Photogrammetric Eng. (June 1960).

[11] E. W. H. Selwyn and J. L. Tearle, The performance of aircraft camera lenses, Proc. Phys. Soc. **LVIII** (493) 1946.

(Paper 64C3–39)